Hindawi Publishing Corporation
ISRN Materials Science
Volume 2014, Article ID 521701, 10 pages
http://dx.doi.org/10.1155/2014/521701

Research Article

Stress and Grain Boundary Properties of GaN Films Prepared by Pulsed Laser Deposition Technique

D. Ghosh,[1] S. Hussain,[2] B. Ghosh,[1] R. Bhar,[1] and A. K. Pal[1]

[1] *Department of Instrumentation Science, Jadavpur University, USIC Building, Calcutta 700 032, India*
[2] *UGC-DAE CSR, Kalpakkam Node, Kokilamedu 603104, India*

Correspondence should be addressed to A. K. Pal; msakp2002@yahoo.co.in

Received 9 January 2014; Accepted 12 February 2014; Published 17 March 2014

Academic Editors: Z. Jiang and N. Martin

Polycrystalline gallium nitride films were successfully deposited on fused silica substrates by ablating a GaN target using pulsed Nd-YAG laser. Microstructural studies indicated an increase in the average crystallite size from ~8 nm to ~70 nm with the increase in substrate temperature from 300 K to 873 K during deposition. The films deposited here were nearly stoichiometric. XPS studies indicated two strong peaks located at ~1116.6 eV and ~395 eV for $Ga2p_{3/2}$ and a N1s core-level peak, respectively. The films deposited at substrate temperature above 573 K are predominantly zinc blende in nature. PL spectra of the films deposited at higher temperatures were dominated by a strong peak at ~3.2 eV. FTIR spectra indicated a strong and broad absorption peak centered ~520 cm^{-1} with two shoulders at ~570 cm^{-1} and 584 cm^{-1}. Characteristic Raman peak at ~531 cm^{-1} for the A_1(TO) mode is observed for all the films. Grain boundary trap states varied between 3.1×10^{15} and 7×10^{15} m^{-2}, while barrier height at the grain boundaries varied between 12.4 meV and 37.14 meV. Stress in the films decreased with the increase in substrate temperature.

1. Introduction

Gallium nitride (GaN) is a promising material for applications in optoelectronic devices, such as ultraviolet-blue-green light-emitting diodes (LEDs) and laser diodes (LDs), due to its direct wide band gap and good thermal stability. It is equally suitable for high-temperature and high-power electronic applications. Depending on the growth conditions, GaN crystallizes either in the stable hexagonal (wurtzite, α-phase) or metastable cubic (zinc-blende, β-phase) polytypes. The prevalent deposition techniques for depositing GaN thin films are mainly metal-organic chemical vapor deposition (MOCVD) and molecular beam epitaxy (MBE). Recently, amorphous and polycrystalline GaN thin films deposited using magnetron sputtering technique [1–7] and laser ablation [8–10] technique have also been reported.

GaN thin films with wurtzite structure were deposited by Chen et al. [5] by using reactive DC magnetron sputtering technique. The films exhibited a polycrystalline structure with a strong (002) orientation and were utilized as active channel layer to produce top-gate n-type thin-film transistors (TFTs). Highly textured polycrystalline GaN films having an average grain size of several hundred angstroms were obtained by Christie et al. [7] using an RF plasma-assisted molecular beam epitaxy system on quartz substrates. Zou et al. [6] reported the deposition of GaN films on glass substrates by the middle frequency magnetron sputtering method. Amorphous gallium nitride (a-GaN) films with thicknesses of 5 and 300 nm were deposited by Wang et al. [8] on n-Si (100) substrates by pulsed laser deposition (PLD), and their field emission (FE) properties were reported. Hong et al. [9] reported the deposition of GaN films on Si (400) wafers by a pulsed laser deposition technique. They observed that although the film and the substrate did not have any interface epitaxy, out-of-plane texture of the film was controllable. Lopez et al. [10] reported a process to produce GaN films activated with Eu^{3+} ions by the pulsed laser deposition (PLD) technique. The film was found to contain submicron size crystals with hexagonal shape. Sanguino et al. [11] deposited GaN thin films on prenitridated c-plane sapphire at two substrate temperatures (600°C and 650°C) by cyclic pulsed laser deposition. Increase in the surface mobility

for a better crystal growth was associated with increasing substrate temperature during deposition. Tong et al. [12] deposited GaN thin films on Si (111) substrates using PLD assisted by gas discharge. The structure, surface morphology, and optoelectronic properties of the films were found to be strongly dependent on the substrate temperature and the laser incident energy.

One of the current issues in GaN research is to deposit high quality GaN polycrystalline thin films using inexpensive substrate and at a relatively lower substrate temperature. Trap states at the grain boundary region and residual stress would modulate the electron transport process in these polycrystalline films. Excepting the attempt made by Chowdhury et al. [3] on Be-doped polycrystalline GaN films, none of the above reports addressed the grain boundary phenomena associated with GaN polycrystalline films adequately. The density of trap states at the grain boundary ($Q_t \sim 1 \times 10^{15}\,\mathrm{m}^{-2}$) and the barrier height ($E_b \sim 1.6\,\mathrm{eV}$) reported by Chowdhury et al. were significantly higher than those one would expect for a good device material. However, they did not report the stress content in the films. Hence, it is apparent that the information on GaN in polycrystalline thin film form reported so far is far from being comprehensive and complete. Thus, there exists still a definite need to synthesize polycrystalline GaN films by appropriate deposition technique so that films containing lesser amount of density of trap states with associated lower barrier height and stress can be achieved. This would ensure unhindered electron transport in the device grade material thus synthesised.

A successful attempt of synthesizing GaN in polycrystalline form by ablating GaN (99.995%) target under controlled deposition condition is reported here. The synthesized films were characterized by measuring optical, microstructural, photoluminescence, and compositional properties. Information related to stress and grain boundary properties has also been documented.

2. Experimental Details

A PLD system evacuated to a level of 10^{-7} Torr was used to ablate a GaN target (99.99% purity, Sigma Aldrich) by using a Nd:YAG laser (wavelength (λ) = 355 nm, pulse duration (τ) = 10 ns, frequency (f) = 10 Hz) for depositing GaN films on fused silica (quartz) and Si (100) substrates (for FTIR measurements). GaN films were deposited at four different substrate temperatures: 473 K, 673 K, 773 K, and 873 K. Time of deposition for all the films was ~9 minutes. The laser fluence was maintained at 8 J/cm^2 and the laser beam was focused with an f = 23 cm glass lens on the target at an angle of 45°, with respect to the normal. The target was rotated at 10 rpm to avoid fast drilling. The distance between the target and the substrate was maintained at ~6.5 cm.

Compositional information was obtained by EDAX (Oxford Instruments' INCA Energy 250 Microanalysis System) and Photoelectron Spectroscopy (XPS). XPS measurements were carried out using a M/s SPECS (Germany) make spectrometer. Al-Kα linewas used as the X-ray source at 1486.74 eV. The anode was operated at a voltage of 15 kV and source power level was set to 400 W. An Ar ion source was also provided for sputter-etch cleaning of specimens. It was operated at 2 kV and 50 μA. This value varied depending on the sample. Spectra were collected using the DLSEGD-PHOIBOS-HSA3500 analyzer. The surface morphology of the films was studied by Field Emission Scanning Electron Microscope (FESEM) (Carl Zeiss SUPRA 55). X-ray diffraction (XRD) studies were carried out by using Rigaku MiniFlex XRD (0.154 nm Cu K$_\alpha$ line) to obtain the microstructural information. Photoluminescence (PL) measurements were recorded at 300 K by using a 300 W xenon arc lamp as the emission source. A Hamamatsu photomultiplier along with a 1/4 m monochromator was used as the detecting system. FTIR spectra were recorded in the range of 400–4000 cm^{-1} by using a Nicolet-380 FTIR spectrometer. Raman spectra were recorded using Renishaw inVia micro-Raman spectrometer using 514 nm Argon laser.

3. Results and Discussion

3.1. Microstructural Study. GaN films were deposited on fused silica substrates and Si (100) substrate at different substrate temperature (T_s). The FESEM pictures of four representative films deposited at 473 K, 673 K, 773 K, and 873 K are shown in Figures 1(a)–1(d), respectively. The FESEM images (Figures 1(a)–1(d)) reveal that the films are compact with well-dispersed polycrystals constituting the films. It was observed that the grain sizes (D) increased (inset of Figure 1(b)) with the increase in substrate temperatures during deposition. The grain size varied between 8 nm to 70 nm with increasing substrate temperature. It may be indicated here that the films grown here are compact and the grain size obtained for these films was significantly larger than those reported for GaN polycrystalline films prepared by sputtering technique [3]. Hong et al. [9] reported a grain size ~100–300 nm for the GaN films deposited by PLD technique on Si (400) wafers kept at 900°C. Comparing the substrate temperature during deposition, grain size obtained here compares favorably with those obtained by Hong et al. The grain size of the films reported in this communication is larger than that reported by Lopez et al. [10] for the Eu^{3+} doped GaN thin films grown on (0001) oriented Al_2O_3 substrates by the PLD growth technique.

A representative histogram of a film deposited at 873 K is shown in the inset of Figure 1(d) which shows a narrow distribution of the grain size. Gradual increase in grain size was observed for films as the substrate temperature was increased from 300 K to 623 K after which rapid grain growth was observed. XRD pattern of a representative GaN film deposited at T_s = 773 K is shown in the inset of Figure 1(c). It may be mentioned here that the XRD patterns are dominated by sharp peaks corresponding to reflections from (101), (102), and (004) planes of GaN. The peak at ~73° became sharper for films deposited at 873 K at the expense of other peaks. This would mean that films deposited above 773 K became preferentially oriented in (004) direction.

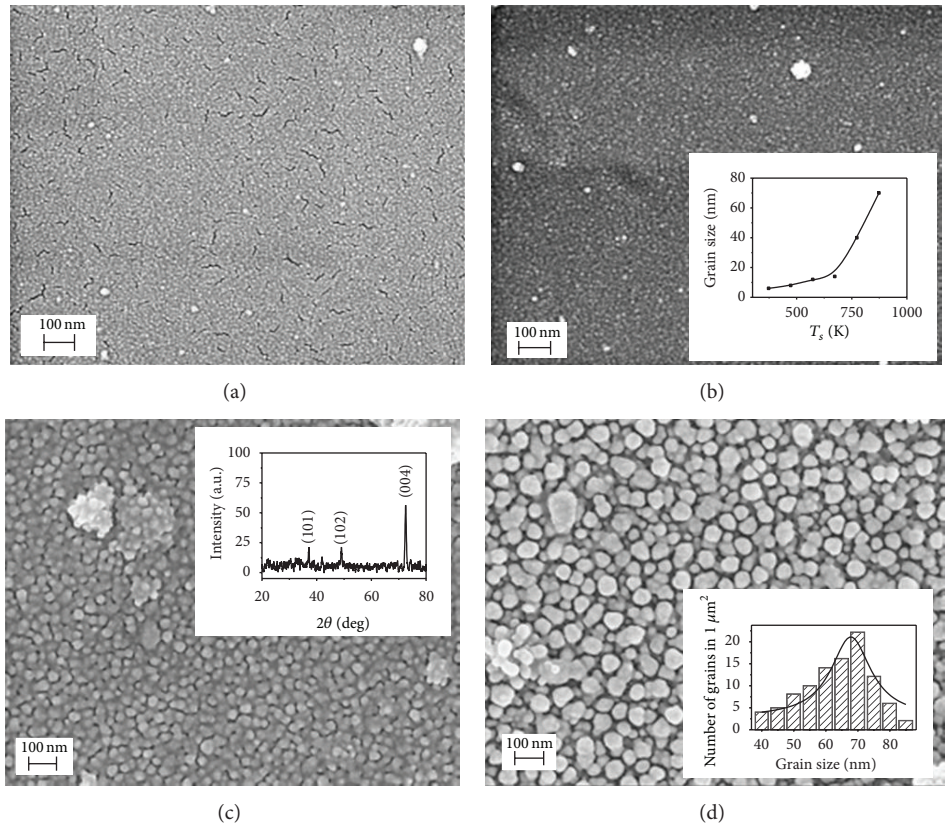

Figure 1: FESEM pictures for four representative GaN films deposited at T_s: (a) 473 K, (b) 673 K (inset shows the variation of grain size with substrate temperature), (c) 723 K (inset shows the corresponding XRD trace), and (d) 873 K (inset shows the corresponding grain size distribution).

3.2. XPS Studies. Figure 2(a) shows the general survey XPS spectrum of a representative GaN film deposited at 873 K. The general survey scans of all the films were found to be the same. A low intense peak for C1s could be located at ~288.03 eV. This is shifted by ~3.63 eV from its standard value towards higher binding energy. The survey scan is dominated by two strong peaks at ~1117 eV (Figure 2(b)) and 1143.7 eV (Figure 2(c)) for $Ga2p_{3/2}$ and $Ga2p_{1/2}$ core-level spectra, respectively [13, 14]. The above intense peak ~1117 eV would correspond to Ga–N bond in GaN. There are a few lower intensity peaks for $Ga3d_{5/2}$ and $Ga3p_{1/2}$ at ~21 eV and 107 eV, respectively. The peak at 107 eV could be deconvoluted (inset of Figure 2(c)) in two peaks located at ~116.2 eV and 109.5 eV. The peak at ~116.2 eV could be identified as arising due to $Ga3p_{1/2}$ and the peak at ~109.5 eV is due to $Ga3p_{3/2}$. The peak ~537 eV overlaps with that of O1s. Oxygen peak arises due to physisorbed oxygen at the surface. Low intensity peak of N1s around ~395 eV is also observed (Figure 2(d)). This peak is associated with the binding energies of N as Ga–N [15].

3.3. Photoluminescence Studies. PL spectra recorded at 80 K and at an excitation of 3.4 eV for the films deposited at 473 K and 873 K are shown in Figures 3(a) and 3(b), respectively. PL spectra for films deposited at lower substrate temperatures (Figure 3(a)) contained three peaks located at ~3.2 eV, 2.91 eV, and ~2.63 eV, while films deposited above 773 K indicated a single peak at ~3.2 eV (Figure 3(b)). The peak at ~3.2 eV could be associated with near band edge luminescence, while the luminescence peaks at ~2.63 eV and 2.91 eV for films deposited at lower substrate temperatures could be identified due to transitions between deep donor and shallow acceptor pairs. The origin of the deep donor may be due to nitrogen vacancy or Ga interstitial site-related defects. The deep acceptor levels arise due to Ga vacancy (V_{Ga}) or gallium vacancy with oxygen on a nitrogen site complex.

3.4. Band Gap and Optical Constants. The absorption coefficients (α) of GaN films were determined by measuring transmittance and reflectance in these films [16, 17]. Films deposited at higher substrate temperature were more absorbing (Figure 3(c)) than those deposited at lower temperatures. This may be due to compactness of the films and lesser number of trap states at the grain boundaries. The absorption coefficient (α) may be written as a function of the incident photon energy ($h\nu$) as follows:

$$\alpha = \left(\frac{A}{h\nu}\right)\left\{h\nu - E_g\right\}^m, \quad (1)$$

where A is a constant and varies for different transitions indicated by different values of m and E_g is the corresponding band gap of the material.

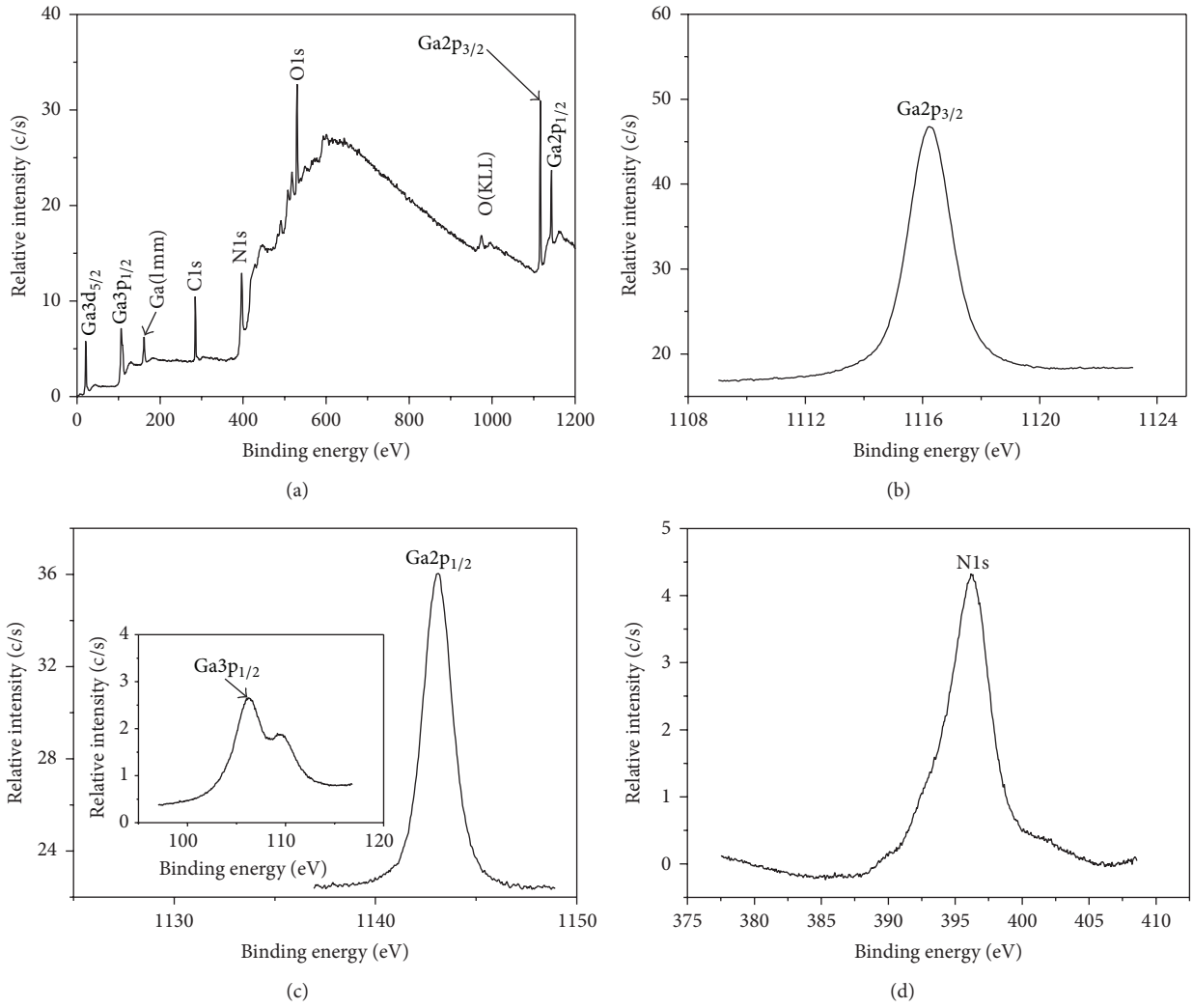

FIGURE 2: XPS spectra of a representative GaN film deposited at 873 K: (a) general survey, (b) $Ga2p_{3/2}$ core-level spectra, (c) $Ga2p_{1/2}$ core-level spectra (inset shows the spectra for $Ga3p_{1/2}$), and (d) N1s core-level spectra.

Now, (1) may be rewritten as

$$\ln(\alpha h\nu) = \ln A + m \ln\left(h\nu - E_g\right), \tag{2}$$

$$\left[\frac{d(\ln \alpha h\nu)}{d(h\nu)}\right] = \frac{m}{h\nu - E_g}. \tag{3}$$

Equation (3) indicates that a plot of $d[\ln(\alpha h\nu)]/d[h\nu]$ versus $h\nu$ will show a divergence at $h\nu = E_g$ from which a rough estimate of E_g may be obtained and as such by using (2), the value of m can easily be evaluated from the slope of the plot of $\ln(\alpha h\nu)$ versus $\ln(h\nu - E_g)$. Figure 3(d) (inset) shows the plot of $\ln(\alpha h\nu)$ versus $\ln(h\nu - E_g)$ for a representative film deposited at 873 K. The value of m was obtained from the slope ~0.51 which indicates a direct transition to be present in the film. The band gap was determined by extrapolating the linear portion of the plot of $(\alpha h\nu)^2$ versus $h\nu$ (Figure 3(d)) and was calculated to be ~3.27 eV. The band gaps obtained for films deposited at different substrate temperatures (T_s) are shown in Table 1 and the variation of E_g with T_s is shown in the inset of Figure 3(c). It could be observed that the films deposited at temperatures higher than 573 K had band gap ~3.2 eV to 3.27 eV. Films deposited at lower temperatures indicated gradual increase in band gap ~2.9 eV to 3.11 eV. It may be noted here that the fall in the transmittance versus wavelength curve (not shown here) was sharper for films deposited at higher substrate temperatures.

The optical constants (refractive index n and extinction coefficient k) of the polycrystalline GaN films were determined from the transmittance versus wavelength traces by using the Kramers-Kronig (KK) model [18] and the modified KK model given by Xue et al. [19]. Using the values for the real part of the refractive index (n) and the extinction coefficient (k), the real and complex part of the dielectric constant (ε_1 and ε_2, resp.) can be estimated by using the relations:

$$\begin{aligned} \varepsilon_1 &= n^2(\lambda) - k^2(\lambda), \\ \varepsilon_2 &= 2n(\lambda)\, k(\lambda). \end{aligned} \tag{4}$$

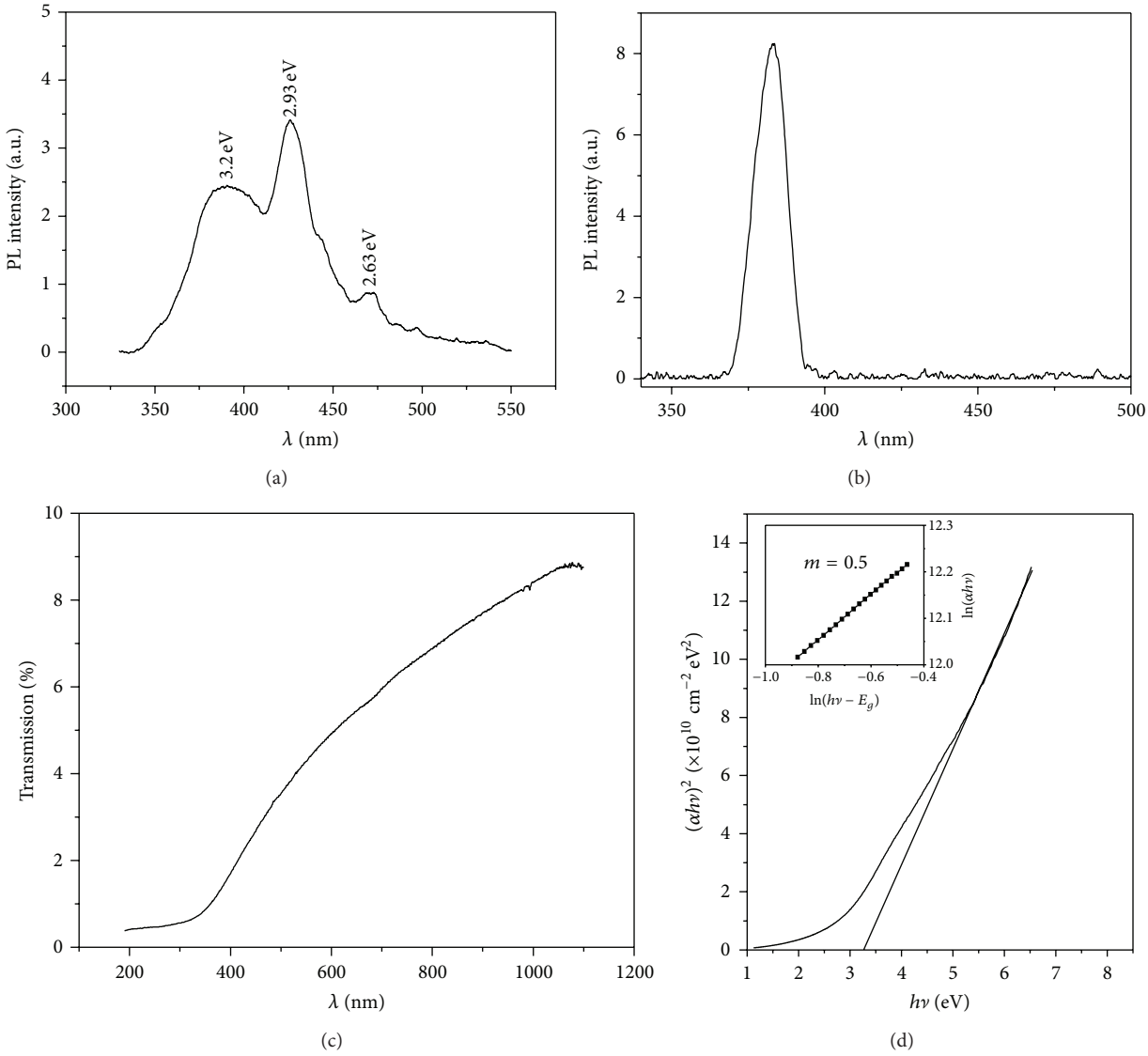

Figure 3: PL spectra for films deposited at (a) 473 K and (b) 873 K, (c) transmittance (T_r) spectra, and (d) plots of $(\alpha h\nu)^2$ versus $h\nu$ for a representative GaN film deposited at 873 K. Inset of (c) shows variation of band gap (E_g) with substrate temperature (T_s) and inset of (d) shows the plot of $\ln(\alpha h\nu)$ versus $\ln(h\nu - E_g)$.

The values of n and k obtained as above are shown in Figures 4(a) and 4(b), respectively. The refractive indices for these GaN films were found to vary from 2.05 to 2.35 within the measured energy range. Their dielectric constant varied from 3.75 to 5.5 as shown in Figures 4(c) and 4(d).

3.5. FTIR and Raman Studies. FTIR spectra for all the films deposited at different substrate temperatures on Si (100) were found to be dominated by a strong and broad absorption peak centered ~520 cm^{-1} with two shoulders at ~570 cm^{-1} and 584 cm^{-1}. Figure 5(a) shows the FTIR spectra for a representative polycrystalline GaN films deposited at T_s = 873 K. The broad peak ~520 cm^{-1} may be ascribed to the presence of peaks due to Ga–N stretching mode at ~570 cm^{-1} and E_1(LO) phonon or A_1(LO) phonon mode at ~584 cm^{-1} [20]. In addition to these peaks, presence of absorption peaks at ~990 cm^{-1} and 1521 cm^{-1} could be due to the Si–O bonds originating from the substrate (silicon).ss.

Raman spectra for a mixed cubic and hexagonal GaN are generally governed by the relations between the phonon modes of the two modifications. The wurtzite structure of GaN arises from the zincblende structure by compressing the crystal along the (111) axis which becomes the c-axis of the hexagonal phase. Also, it may happen that changing the stacking of layers along this axis would result in a doubling of the number of atoms in a primitive unit cell. This would culminate in splitting of T_2 mode of the cubic phase into the A_1 and E_1 modes of the hexagonal phase. Since the hexagonal distortion is small, the above splitting will also be generally small.

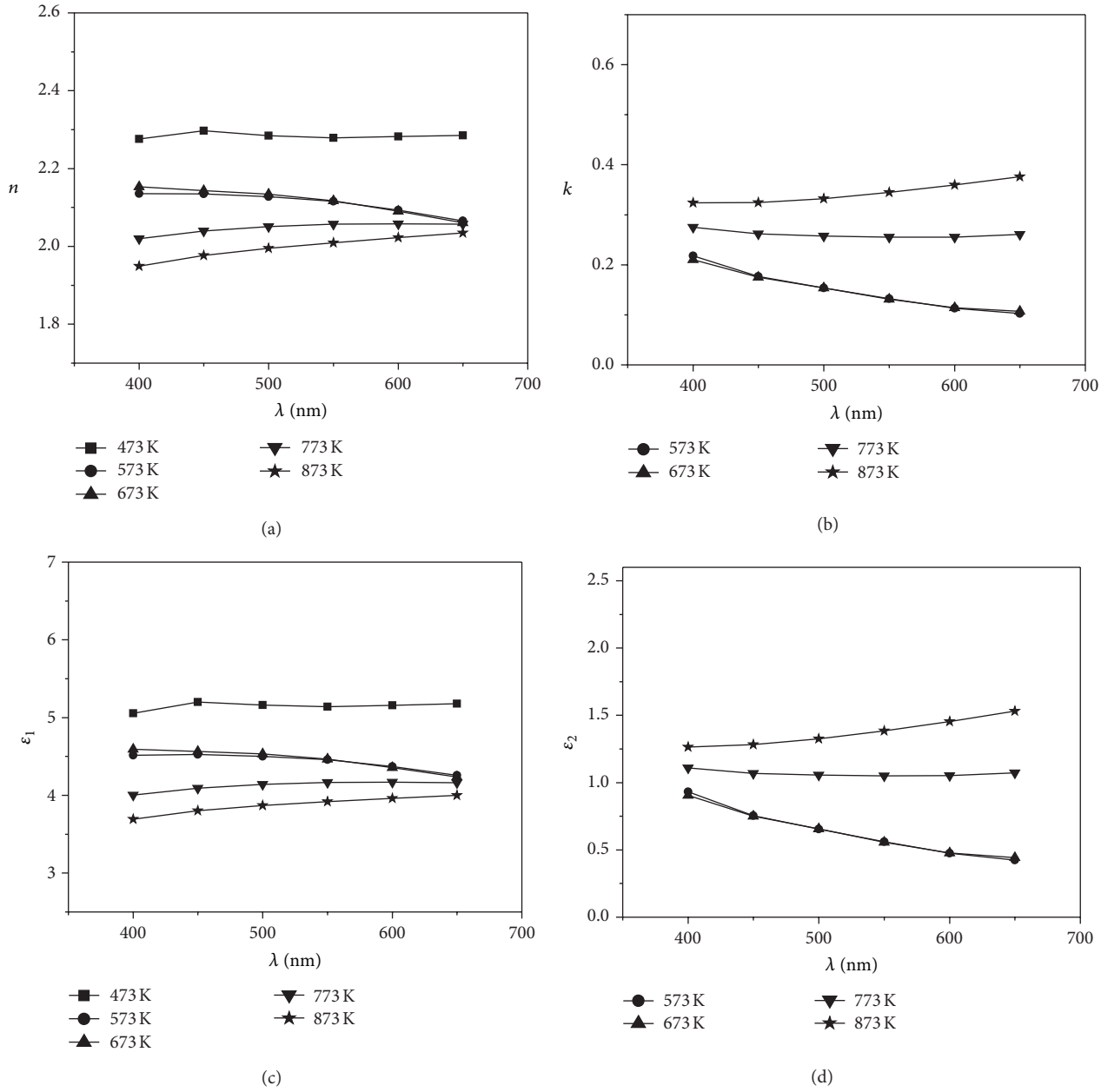

FIGURE 4: (a) Plots of n versus λ, (b) plots of k versus λ, (c) plots of ε_1 versus λ, and (d) plots of ε_2 versus λ of a representative GaN film.

GaN films deposited at lower substrate temperatures are predominantly hexagonal in structure and cubic GaN content in the films increases as the deposition temperature is increased. Thus, one would expect relevant signatures in Raman modes in such films. Figure 5(b) shows the Raman spectra of a GaN films deposited at 873 K. The Raman spectrum showed a first-order Raman active phonon mode at ~531 cm^{-1} for A_1(TO) modes. Three broad peaks spreading over 570 cm^{-1} to 680 cm^{-1} have their centers at 571 cm^{-1}, 616 cm^{-1}, and 644 cm^{-1}, corresponding to the first order high frequency E_2, overtone of E_1(TO), and A_1(TO) overtone modes, respectively. The strongest E_2 (high) phonon line in the spectrum reflects the characteristics of the hexagonal crystal phase of the GaN film. The Raman peak at 672 cm^{-1} would arise from the optical-phonon branch at the zone boundary.

It is known that at high defect densities wave vector conservation in the Raman scattering process breaks down and phonons from the entire Brillouin zone can be observed in the Raman spectrum [21]. Thus, the Raman spectrum would reflect the total phonon density of states due to disorder-activated Raman scattering (DARS). The Raman peak at 672 cm^{-1} probably arises from the optical-phonon branch at the zone boundary. Siegle and coworkers [22] have reported second-order Raman scattering experiments on hexagonal and cubic GaN covering the acoustic

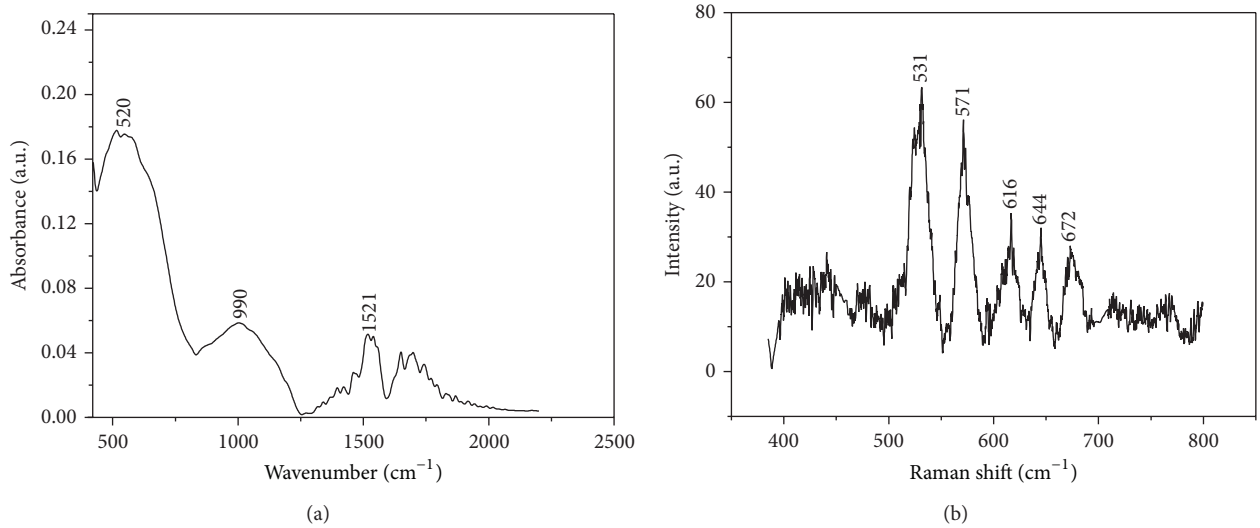

Figure 5: (a) FTIR and (b) Raman spectra of a representative GaN film deposited at 873 K.

and the optical overtone spectral region. The hexagonal modes lying between the first-order peaks at ~616 cm^{-1} and ~644 cm^{-1} could be attributed to the overtone processes of the highest acoustic-phonon branch either at the zone boundary (L point) or from the B mode at the Γ point.

3.6. Grain Boundary Studies from Below-Band-Gap Absorption Studies. GaN films deposited here could be seen to consist of aggregates of randomly distributed grains and grain boundary regions. Size of the grains increased as the substrate temperature during deposition was increased (inset of Figure 1(b)). The grain boundary region would contain a large amount of defect states which become charged after trapping free carriers from the neighbouring grains. In addition to these intrinsic defect states at the grain boundary regions of the GaN films, a considerable amount of thermal stress due to the mismatch of thermal expansion coefficients of the film (α_{film}) and substrate (α_{subs}) is bound to appear in these films. This would result in fluctuating nature of the potential [23–25]. The band gap (E_g) would in turn also have a fluctuating nature. This would result in additional indirect optical transitions below the fundamental band gap of the material. The details of the processes have already been reported elsewhere [23–25]. Following the detailed procedure reported by Maity et al. [23], the relevant grain boundary parameters like density of trap states (Q_t) and barrier height at the grain boundary (E_b) were computed from the theoretical fit of normalized absorption coefficients α/α_0 below the band gap region.

Figure 6(a) shows representative plots of the experimental data of normalized absorption coefficients α/α_0 for a representative GaN film deposited at 873 K. It may be mentioned here that the contribution due to the thermal disorder at a specific temperature (at which the optical absorption has been recorded) is fixed, the ultimate shape of α/α_0 versus $(E_g - h\nu)$ plot will depend on the amount of the intrinsic disorder or the density of the defect states present in the film. The grain boundary parameters (Q_t and E_b) were estimated from the best fit theoretical curve (shown in Figure 6(a)) corresponding to the experimental data of α/α_0 versus $(E_g - h\nu)$, α_0 being the value of α at E_g. The values of Q_t and E_b are given in Table 1.

Variation of Q_t and E_b with grain size (i.e., with substrate temperature during deposition) is depicted in Figure 6(b). It could be observed that the density of trap states (Q_t) at the grain boundaries decreased from 7×10^{15} m^{-2} to 3.1×10^{15} m^{-2} for films deposited at higher temperatures. These values are smaller than those reported for the rf sputtered films [3]. The barrier height at the grain boundaries (E_b) was significantly smaller compared to those reported by Chowdhury et al. [3]. As the films are high resistive, the number density of charge carriers will be small. The films would be fully depleted of charge carriers when the density of trap states at the grain boundaries is large for films deposited at lower temperatures. As the number density of trap states decreased for films deposited at higher substrate temperatures, probability of the trap states to get fully filled by the charge carriers will increase leaving behind the grains partially depleted. This has been reflected by the exponential fall in E_b with the grain size.

3.7. Determination of Stress. Earlier reports by various workers indicated that the material properties (e.g., stress, strain, and barrier height) are very much influenced by the presence of trap states at the grain boundaries which are, in fact, highly insulating regions. The details of the technique have already been discussed elsewhere [24]. It has been observed in the earlier section that grain boundaries in polycrystalline GaN films effectively control the electron transport as well as optical absorbance. Besides the above grain boundary effects, mechanical stress due to lattice dilation was seen to modulate the lattice ordering at the grain and grain boundary region. This would modulate the below-band-edge optical absorption processes as a whole in the form of electrostatic

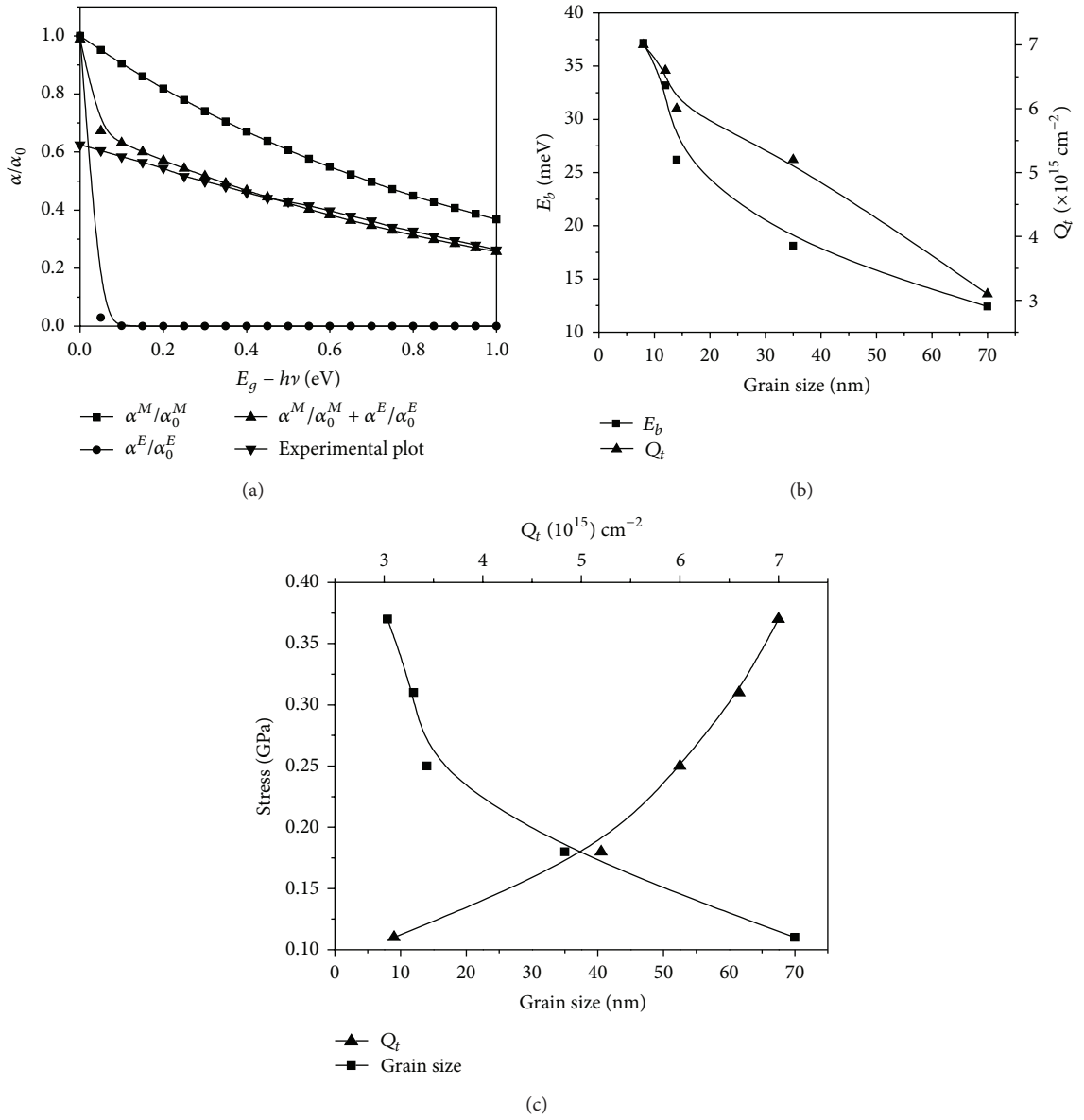

FIGURE 6: (a) Variation of α/α_0 versus $(E_g - h\nu)$ for a representative GaN film deposited at 873 K. -▲-: theoretical best fit curves. (b) Variation of trap state density (Q_t) and barrier height (E_b) with grain size and (c) variation of stress (S) with grain size (—■—) and density of trap state (Q_t) (—▲—) at grain boundary region for GaN films deposited at 873 K.

fluctuations of the band edge [26–28] and hence information on the stress could also be generated from the above.

The disorders in the film would result in considerable amount of indirect optical transitions for photon energy $h\nu < E_g$ which in turn would produce a broad absorption band tail, in contrast to the sharp absorption edge produced in a single-crystalline material. The specific shape of the absorption band tail which depends on the initial and final states of the transitions concerned will be determined by the intrinsic strain $(\delta a/a)_{gb}$. The intrinsic strain could be determined by the density of the defect states at the grain boundary region of the film since the other contributions in the total strain would remain constant for a particular substrate material at a specific temperature.

Now, considering contributions from both the thermal and grain boundary effects the strain $(\delta a/a)$ and stress (S) in the GaN films may be expressed as

$$\left(\frac{\delta a}{a}\right)_{\text{total}} = \left(\frac{\delta a}{a}\right)_{\text{gb}} + \left(\frac{\delta a}{a}\right)_{\text{th}},$$
$$S_{\text{total}} = S_{\text{gb}} + S_{\text{th}}. \tag{5}$$

Here, S_{gb}, $(\delta a/a)_{gb}$, and S_{th}, $(\delta a/a)_{th}$ correspond to the grain boundary and thermal components of stress and strain,

Table 1: Different quantities related to GaN films obtained from this study.

Sample number and substrate temperature (T_s)	E_g (eV)	Grain size from SEM (nm)	Λ_d (nm)	Q_t (10^{15} m^{-2})	E_b (meV)	Stress (GPa)
GaN-1 473 K	2.90	8	38.3	7	37.2	0.37
GaN-2 573 K	3.11	12	35.5	6.6	33.2	0.31
GaN-3 673 K	3.21	14	33.2	6.0	26.2	0.25
GaN-4 773 K	3.24	35	30.4	5.2	18.1	0.17
GaN-5 873 K	3.27	70	28.9	3.1	12.4	0.11

respectively. The thermal stress arises when the film is cooled after deposition. The stress due to grain boundaries will, in general, be proportional to the total grain boundary area which in turn would depend inversely on the average grain size [25, 28, 29]. We have considered the lattice dilation at finite temperature as due to phonon vibration and defect states in the polycrystalline GaN films [23, 25, 27].

From the experimentally obtained values of residual strain ($\delta a/a$) obtained as above and by knowing the standard values of Young's modulus Y (GPa) and the Poisson's ratio (γ) for a given film material, the true stress (S) can be obtained from (6) as shown below:

$$S = \left[\frac{Y}{1-\gamma}\right]\left(\frac{\delta a}{a}\right). \quad (6)$$

Stresses in the films thus evaluated are shown in Figure 6(c). It may be noted that the stress decreased from 0.38 GPa to 0.1 GPa for films deposited at higher temperature, that is, with increase in grain size (Table 1 and Figure 6(c)). This result is in commensurate with the fact that, at a reasonable deposition rate, the adatoms will have increased mobility with increased substrate temperature during deposition to facilitate grain growth. Further, with increased grain size, grain boundaries would decrease resulting in decrease in the density of trap states.

4. Conclusion

Polycrystalline films of GaN were deposited with different grain sizes by varying the substrate temperature during pulse laser deposition. Grain size varied between 8 to 70 nm as the substrate temperature during sputtering changed from 300 K to 873 K. XPS studies indicated two strong peaks located at ~1116.6 eV and ~395 eV for $Ga2p_{3/2}$ and N1s core-level spectra, respectively. Photoluminescence measurement at 300 K exhibited a strong peak at ~2.91 eV followed by a low intensity peak for band edge luminescence at ~3.20 eV. The luminescence at ~2.63 eV could be identified due to transitions between deep donor and shallow acceptor pairs. FTIR spectra were dominated by a strong and broad absorption peak centered ~520 cm^{-1} with two shoulders at ~570 cm^{-1} and 584 cm^{-1}. First-order Raman active phonon mode at ~513 cm^{-1} for A_1(TO) modes was observed. Additionally, three broad peaks spreading over 570 cm^{-1} to 680 cm^{-1} that appeared in Raman spectra have their centers at 570 cm^{-1}, 614 cm^{-1}, and 644 cm^{-1}, corresponding to the first-order high frequency E_2, overtone of E_1(TO), and A_1(TO) overtone modes, respectively. Density of trap states at the grain boundary (Q_t) changed from 7×10^{-15} m^{-2} to 3.1×10^{-15} m^{-2} and the barrier height (E_b) decreased from 37.17 meV to 12.4 meV as the grain size increased with the increase in deposition temperature. The stress decreased from 0.38 GPa to 0.1 GPa for films deposited at higher temperature.

Conflict of Interests

The authors declare that there is no conflict of interests regarding the publication of this paper.

Acknowledgments

The authors wish to thank the Department of Science and Technology, Government of India, for sanctioning financial assistance under PURSE Scheme of Jadavpur University for executing this programme. D. Ghosh and B. Ghosh wish to thank the Department of Science and Technology, Government of India, and UGC-DAE-CSR, respectively, for granting them the fellowships.

References

[1] E. C. Knox-Davies, S. R. P. Silva, and J. M. Shannon, "Properties of nanocrystalline GaN films deposited by reactive sputtering," *Diamond and Related Materials*, vol. 12, no. 8, pp. 1417–1421, 2003.

[2] T. Maruyama and H. Miyake, "Gallium nitride thin films deposited by radio-frequency magnetron sputtering," *Journal of Vacuum Science and Technology A: Vacuum, Surfaces and Films*, vol. 24, no. 4, pp. 1096–1099, 2006.

[3] M. P. Chowdhury, R. K. Roy, B. R. Chakraborty, and A. K. Pal, "Beryllium-doped polycrystalline GaN films: optical and grain boundary properties," *Thin Solid Films*, vol. 491, no. 1-2, pp. 29–37, 2005.

[4] K. Kubota, Y. Kobayashi, and K. Fujimoto, "Preparation and properties of III-V nitride thin films," *Journal of Applied Physics*, vol. 66, no. 7, pp. 2984–2988, 1989.

[5] R. Chen, W. Zhou, and H. S. Kwok, "Top-gate thin-film transistors based on GaN channel layer," *Applied Physics Letters*, vol. 100, no. 2, Article ID 022111, 2012.

[6] C. W. Zou, H. J. Wang, M. L. Yin et al., "Preparation of GaN films on glass substrates by middle frequency magnetron sputtering," *Journal of Crystal Growth*, vol. 311, no. 2, pp. 223–227, 2009.

[7] V. A. Christie, S. I. Liem, R. J. Reeves, V. J. Kennedy, A. Markwitz, and S. M. Durbin, "Characterisation of polycrystalline gallium nitride grown by plasma-assisted evaporation," *Current Applied Physics*, vol. 4, no. 2–4, pp. 225–228, 2004.

[8] F. Y. Wang, R. Z. Wang, W. Zhao, S. XueMei, W. Bo, and Y. Hui, "Field emission properties of amorphous GaN ultrathin films fabricated by pulsed laser deposition," *Science in China, Series F: Information Sciences*, vol. 52, no. 10, pp. 1947–1952, 2009.

[9] J. Hong, Y. Chang, Y. Ding, Z. L. Wang, and R. L. Snyder, "Growth of GaN films with controlled out-of-plane texture on Si wafers," *Thin Solid Films*, vol. 519, no. 11, pp. 3608–3611, 2011.

[10] N. P. Lopez, J. H. Tao, J. McKittrick et al., "Eu^{3+} activated GaN thin films grown on sapphire by pulsed laser deposition," *Physica Status Solidi (C): Current Topics in Solid State Physics*, vol. 5, no. 6, pp. 1756–1758, 2008.

[11] P. Sanguino, M. Niehus, L. V. Melo et al., "Characterisation of GaN films grown on sapphire by low-temperature cyclic pulsed laser deposition/nitrogen rf plasma," *Solid-State Electronics*, vol. 47, no. 3, pp. 559–563, 2003.

[12] X. L. Tong, Q. G. Zheng, S. L. Hu, Y. X. Qin, and Z. H. Ding, "Structural characterization and optoelectronic properties of GaN thin films on Si(111) substrates using pulsed laser deposition assisted by gas discharge," *Applied Physics A: Materials Science and Processing*, vol. 79, no. 8, pp. 1959–1963, 2004.

[13] J. F. Moulder, W. F. Stickle, P. E. Sobol, and K. D. Bomben, *Handbook of X-Ray Photoelectron Spectoscopy*, Edited by J. Chastain, Perkin-Elmer, Eden Prairia, Minn, USA, 1992.

[14] D. Briggs and M. P. Seah, *Practical Surface Analysis*, John Wiley & Sons, New York, NY, USA, 1979.

[15] S. I. Bahn, C. M. Lee, S. J. Lee, J. I. Lee, C. S. Kim, and S. K. Noh, "Determination of the Al mole fraction in epitaxial $AL_XGa_{1-x}N$/GaN ($x < 0.25$) heterostructures," *Journal of the Korean Physical Society*, vol. 43, no. 3, pp. 381–385, 2003.

[16] J. C. Manifacier, J. Gasiot, and J. P. Fillard, "A simple method for the determination of the optical constants n, k and the thickness of a weakly absorbing thin film," *Journal of Physics E: Scientific Instruments*, vol. 9, no. 11, pp. 1002–1004, 1976.

[17] D. Bhattacharyya, S. Chaudhuri, A. K. Pal, and S. K. Bhattacharya, "Bandgap and optical transitions in thin films from reflectance measurements," *Vacuum*, vol. 43, no. 4, pp. 313–316, 1992.

[18] J. I. Pankove, *Optical Processes in Semiconductors* , Prentice-Hall, Englewood Cliffs, NJ, USA.

[19] S. W. Xue, X. T. Zu, W. G. Zheng, H. X. Deng, and Z. Xiang, "Effects of Al doping concentration on optical parameters of ZnO:Al thin films by sol-gel technique," *Physica B: Condensed Matter*, vol. 381, no. 1-2, pp. 209–213, 2006.

[20] M. Mizushima, T. Kato, Y. Honda, M. Yamaguchi, and N. Sawaki, "Infrared reflectance in GaN/AlGaN triangular stripes grown on Si(111) substrates by MOVPE," *Journal of the Korean Physical Society*, vol. 42, pp. S750–S752, 2003.

[21] W. Limmer, W. Ritter, R. Sauer, B. Mensching, C. Liu, and B. Rauschenbach, "Raman scattering in ion-implanted GaN," *Applied Physics Letters*, vol. 72, no. 20, pp. 2589–2591, 1998.

[22] H. Siegle, G. Kaczmarczyk, L. Filippidis, A. P. Litvinchuk, A. Hoffmann, and C. Thomsen, "Zone-boundary phonons in hexagonal and cubic GaN," *Physical Review B—Condensed Matter and Materials Physics*, vol. 55, no. 11, pp. 7000–7004, 1997.

[23] A. B. Maity, S. Chaudhuri, and A. K. Pal, "Modification of the absorption edge due to grain boundaries and mechanical stresses in polycrystalline semiconductor films," *Physica Status Solidi (B)*, vol. 183, no. 1, pp. 185–191, 1994.

[24] A. B. Maity, M. Basu, S. Chaudhuri, and A. K. Pal, "Stress and microhardness in polycrystalline thin films from below-band-gap absorption studies," *Journal of Physics D: Applied Physics*, vol. 28, no. 12, pp. 2547–2553, 1995.

[25] A. B. Maity, D. Bhattacharyya, S. Chaudhuri, and A. K. Pal, "Absorption tail of polycrystalline semiconductor films," *Vacuum*, vol. 46, no. 3, pp. 319–322, 1995.

[26] V. I. Gavrilenko, "Electronic structure and optical properties of polycrystalline cubic semiconductors," *Physica Status Solidi (B)*, vol. 139, no. 2, pp. 457–466, 1987.

[27] J. Szczyrbowski, "On the shape of the absorption tail in amorphous solids," *Physica Status Solidi (B)*, vol. 96, no. 2, pp. 769–774, 1979.

[28] J. Tauc, "Absorption edge and internal electric fields in amorphous semiconductors," *Materials Research Bulletin*, vol. 5, no. 8, pp. 721–729, 1970.

[29] R. W. Hoffman, "Stresses in thin films: the relevance of grain boundaries and impurities," *Thin Solid Films*, vol. 34, no. 2, pp. 185–190, 1976.